

Electronic Supporting Information

for

Fluoride-responsive organogelator based on oxalamide-derived anthraquinone

by

**Zoran Džolić,^a Massimo Cametti,*^b Antonella Dalla Cort,^b
Luigi Mandolini*^b and Mladen Žinić*^a**

^a Department of Organic Chemistry and Biochemistry, Ruđer Bošković Institute, Bijenicka 54,
10000 Zagreb, Croatia.

^b Dipartimento di Chimica and IMC-CNR Sezione Meccanismi di Reazione, Università La
Sapienza, 00185 Roma, Italy.

Table of contents:

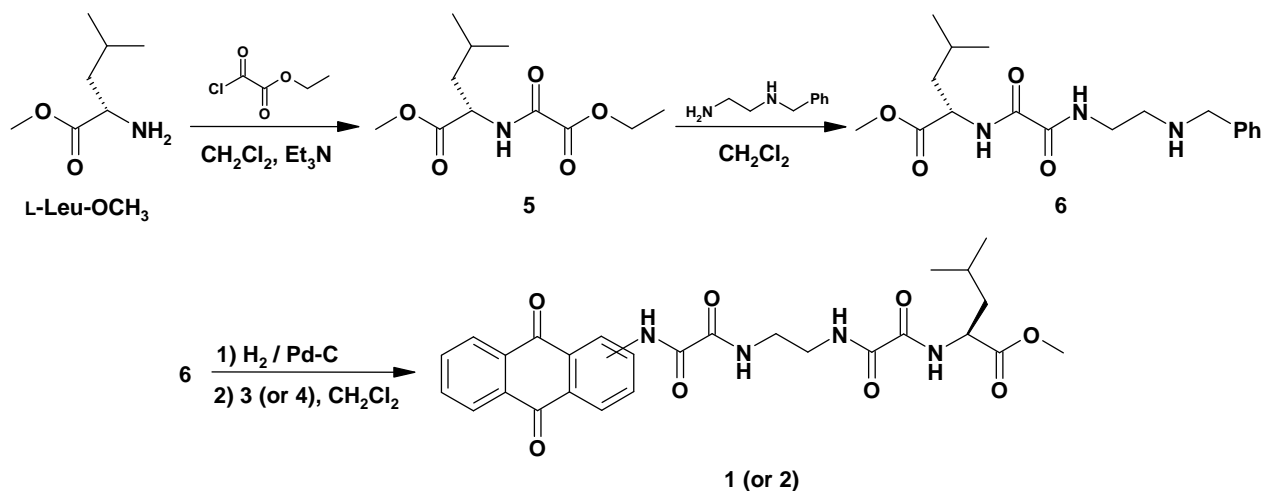
Page numbers:

1. Synthetic procedures for 1 and 2	S3 – S6
2. Temperature dependent absorption spectral changes of gels of 1	S7
3. Colour changes observed for 1	S8
4. Fluoride binding properties of 2	S9
5. Plot of ^1H NMRs on addition of F^-	S10
6. Anion binding properties of 2	S11
7. Minimized structures of 1 and 2	S12
8. Anion binding properties of 3 and 4	S13 – S16
9. Additional reference	S17

Experimental Section

General:

All solvents were purified and dried by standard procedures and distilled prior to use. Melting points were determined on a Kofler hot-stage apparatus and are uncorrected. ^1H and ^{13}C NMR spectra were recorded with a Bruker AV 300 spectrometer. Chemical shifts, in ppm, are referred to TMS as internal standard. FT-IR spectra were recorded on a Perkin-Elmer 297 spectrometer. Optical rotations were measured on an Optical Activity AA-10 Automatic Polarimeter in a 1 dm cell at 589 nm; concentrations were given in g/100 mL. Compounds **3**^{S1} and **4**^{S2} were previously described in the literature.



Scheme 1. Synthesis of anthraquinone derivatives **1** and **2**.

Ethyl *N*-(*L*-Leucine methyl ester)oxalamate (**5**)

Ethyl oxalyl chloride (3.35 mL, 30 mmol) in dry CH_2Cl_2 (20 mL) was added dropwise into a mixture of (*S*)-leucine methyl ester hydrochloride (5 g, 27.5 mmol) and triethylamine (8.1 mL, 58 mmol) in dry methylene chloride (100 mL) over 1 h at 0 °C, and stirred for 18 h at room temperature. The mixture was washed with water (2 x 50 mL), saturated aqueous ammonium chloride (3 x 50 mL), and water again (2 x 50 mL), The organic layer was dried over magnesium sulphate and evaporated to obtain pure **5** as colourless oil (6.2 g, 92%).

mp = oil; $[\alpha]_D^{22} = -10$ ($c = 1.48$ in CH_2Cl_2); $^1\text{H NMR}$ (CDCl_3): $\delta = 7.51$ (d, $J = 8.2$, 2H, NH), 4.65 (m, 1H, C^*H), 4.36 (q, $J = 7.1$, 2H, CH_2), 3.75 (s, 3H, OCH_3), 1.68 (m, 3H, $\text{CH}_\gamma + \text{CH}_{2\beta}$), 1.40 (t, $J = 7.1$, 2H, CH_3), 0.95 (d, $J = 4.7$, 6H, 2 x CH_3); $^{13}\text{C NMR}$ (CDCl_3): $\delta = 14.1, 21.8, 22.9, 24.9, 41.4, 51.3, 52.6, 63.4, 156.3, 160.3, 172.4$; IR (KBr): $\nu = 3344, 2956, 2873, 1747, 1703, 1521 \text{ cm}^{-1}$.

***N*-(L-Leucine methyl ester)-*N'*-(*N*-benzylethyldiamine)oxalamide (6)**

A mixture of **5** (2 g, 8.2 mmol) and *N*-benzylethyldiamine^{S3} (1.37 g, 9.1 mmol) in dry CH_2Cl_2 (50 mL) was stirred overnight at room temperature under an inert atmosphere. After stirring, the solution was washed with water (2 x 20 mL), saturated aqueous ammonium chloride (2 x 20 mL), water (3 x 20 mL), dried over Na_2SO_4 , and concentrated in vacuo. Purification by column chromatography over silica gel ($\text{CH}_2\text{Cl}_2/\text{CH}_3\text{OH}$ 3:1) afforded **6** (2.5 g, 87%) as an oil which solidified after one week.

mp = 39-40 °C; $[\alpha]_D^{22} = -13$ ($c = 1$ in CH_2Cl_2); $^1\text{H NMR}$ (CDCl_3): $\delta = 7.85$ (br t, 1H, NH), 7.75 (d, $J = 8.7$, 1H, NH), 7.31 (m, 5H, -Ph), 4.60 (m, 1H, C^*H), 3.81 (s, 2H, $-\text{CH}_2\text{Ph}$), 3.74 (s, 3H, OCH_3), 3.42 (q, $J = 5.9$, 2H, $-\text{CH}_2$), 2.83 (t, $J = 5.9$, 2H, $-\text{CH}_2$), 1.85 (br s, 1H, NH), 1.67 (m, 3H, $\text{CH}_\gamma + \text{CH}_{2\beta}$), 0.95 (d, $J = 6.2$, 6H, 2 x CH_3); $^{13}\text{C NMR}$ (CDCl_3): $\delta = 21.8, 22.9, 24.9, 39.4, 41.2, 47.5, 51.2, 52.5, 53.4, 127.3, 128.3, 128.6, 139.6, 159.6, 159.8, 172.2$; IR (KBr): $\nu = 3302, 2958, 2871, 1751, 1655, 1518 \text{ cm}^{-1}$.

General procedure for the synthesis of the anthraquinone derivatives 1 and 2:

A solution of **6** (1 g, 2.9 mmol) in dry CH_3OH (50 mL) was hydrogenated over 10% Pd/C (100 mg) at room temperature overnight. The catalyst was removed by filtration through Celite, washed with methanol, and the filtrate evaporated and dried to afford the free amine. The oily product was used for the next reaction without purification.

3 (or **4**) (0.94 g, 2.9 mmol) was dissolved in dry CH_2Cl_2 (50 mL) with stirring, and a solution of the oily product (dissolved in 20 ml of dry CH_2Cl_2) was added. The resulting reaction mixture

was stirred at room temperature for 48 h under N₂. The Precipitate formed was filtered and washed thoroughly with CH₂Cl₂ and recrystallized from DMF.

Compound 1

Yield: 1.18 g (76%) of a yellow solid; mp 282 °C; $[\alpha]_D^{22} = -17$ (c = 0.3 in DMSO); ¹H NMR (DMSO-*d*₆): δ = 13.45 (s, 1H, NH), 9.29 (br t, 1H, NH), 9.06 (t, *J* = 8.3, 1H, Ar-CH), 9.01 (s, 1H, NH), 8.97 (br t, 1H, NH), 8.24 (m, 2H, Ar-CH), 8.00 (m, 4H, Ar-CH), 4.36 (m, 1H, C^{*}H), 3.62 (s, 3H, OCH₃), 3.39 (m, 4H, 2 x -CH₂), 1.83 (m, 1H, CH_γ), 1.53 (m, 2H, CH_{2β}), 0.85 (2d, *J* = 5.9, 6H, 2 x CH₃); ¹³C NMR (DMSO-*d*₆, 353 K): δ = 20.9, 22.1, 24.0, 38.1, 38.6, 39.1, 50.4, 51.4, 122.3, 124.8, 126.0, 126.6, 132.0, 133.3, 133.8, 134.2, 134.3, 135.1, 139.0, 158.9, 159.3, 159.5, 159.6, 171.3, 175.9, 181.6, 185.6; IR (KBr): ν = 3300, 2956, 1750, 1698, 1668, 1657, 1521 cm⁻¹; elemental analysis calcd (%) for C₂₇H₂₈N₄O₈: C 60.44 H 5.26 N 10.44; found C 60.40 H 5.32 N 10.40.

Compound 2

Yield: 1.31 g (84%) of a brown solid; mp 306 °C; $[\alpha]_D^{22} = -13$ (c = 0.3 in DMSO); ¹H NMR (DMSO-*d*₆): δ = 11.30 (s, 1H, NH), 9.21 (br t, 1H, NH), 9.01 (t, *J* = 8.5, 1H, NH), 8.97 (br t, 1H, NH), 8.81 (s, 1H, Ar-CH), 8.25 (m, 4H, Ar-CH), 7.93 (m, 2H, Ar-CH), 4.36 (m, 1H, C^{*}H), 3.63 (s, 3H, OCH₃), 3.37 (m, 4H, 2 x -CH₂), 1.82 (m, 1H, CH_γ), 1.55 (m, 2H, CH_{2β}), 0.85 (2d, *J* = 5.9, 6H, 2 x CH₃); ¹³C NMR (DMSO-*d*₆): δ = 21.0, 22.5, 24.1, 38.2, 38.7, 39.0, 50.4, 51.7, 125.2, 126.4, 126.5, 127.9, 128.8, 132.9, 133.0, 133.9, 134.0, 134.3, 143.0, 159.1, 159.6, 159.7, 159.8, 171.0, 171.7, 181.2, 182.1; IR (KBr): ν = 3309, 2956, 1748, 1670, 1654, 1592, 1515 cm⁻¹; elemental analysis calcd (%) for C₂₇H₂₈N₄O₈: C 60.44 H 5.26 N 10.44; found C 60.50 H 5.30 N 10.39.

Gelation test: A weighed amount of gelator (3 mg) was mixed with a small amount of DMF (100 μL) in a test tube (inside diameter 10 mm) and the mixture was gently heated until the solid was dissolved. To the resulting solution measured volumes (100 – 500 μL) of a selected solvent were repeatedly added. After each addition, the mixture was heated until the substance dissolved, and then allowed to cool spontaneously to room temperature. The gel formation was checked by

test tube inversion. When the compound did not dissolve completely, it was labelled as “insoluble”, whereas “precipitation” indicates that reprecipitation occurred with cooling.

TEM measurements: A piece of a *p*-xylene gel was placed on a carbon-coated copper grid and removed after 1 min, leaving some small patches of the gel on the grid. After drying at low pressure, the samples were shadowed at an angle of 20° with palladium. The samples were examined with a FEI MORGAGNI 268D transmission electron microscope operating at 70 kV.

AFM measurements: Atomic Force Microscopy images were recorded under ambient conditions using a Digital Instrument Multimode Nanoscope IIIa operating in the tapping mode regime. AFM samples were prepared by drop casting a dilute solution of nanostructures (5.0 μL of EtOH and *p*-xylene gels suspended in 0.100 ml of EtOH and *p*-xylene) on freshly cleaved mica (Ted Pella).

Optical measurements: Electronic absorption spectra were recorded on Perkin Elmer Lambda 18 spectrophotometer. Temperature dependent studies were carried out in a 1 cm quartz cuvette with the thermistor directly attached to the wall of the cuvette holder. The UV-Vis spectra of the sensors in the presence of analytes were recorded as increasing amounts of analytes were added in DMSO. All anions used were F⁻, Cl⁻, Br⁻, I⁻, H₂PO₄⁻ and CH₃CO₂⁻ in the form of their tetrabutylammonium salts. Titration plots were generated by using Sigmaplot 8.0.

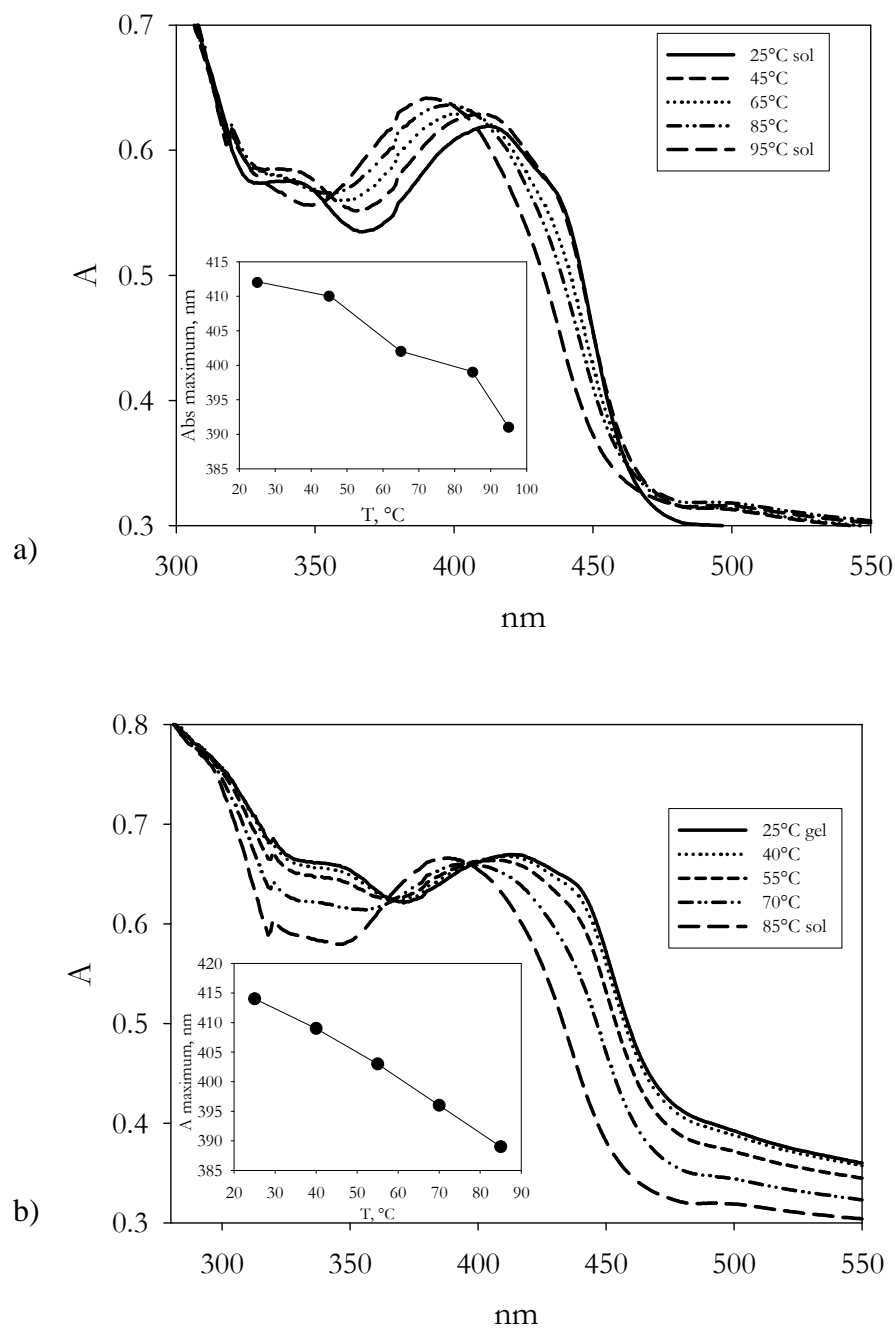


Figure S1: Temperature dependent absorption spectral changes of a) **1**-EtOH gel (25 ° - 95 °C) (inset: changes on the absorption maximum at 412 nm) and b) **1**-*p*-xylene gel (inset: changes on the absorption maximum at 414 nm).

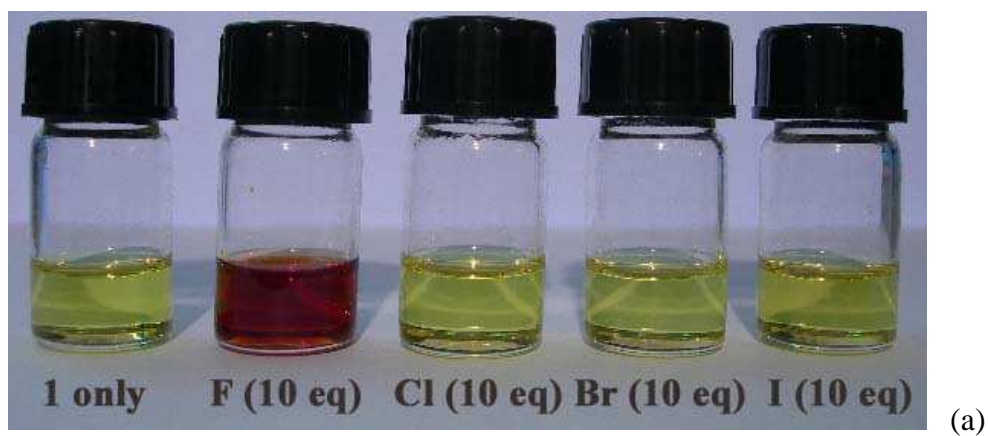


Figure S2: Colour changes observed for **1** in DMSO (1×10^{-3} M) upon addition of anions as tetrabutylammonium salts at room temperature (a) and (b) colour change observed for **1** in DMSO (1×10^{-4} M) upon addition of tetrabutylammonium fluoride .

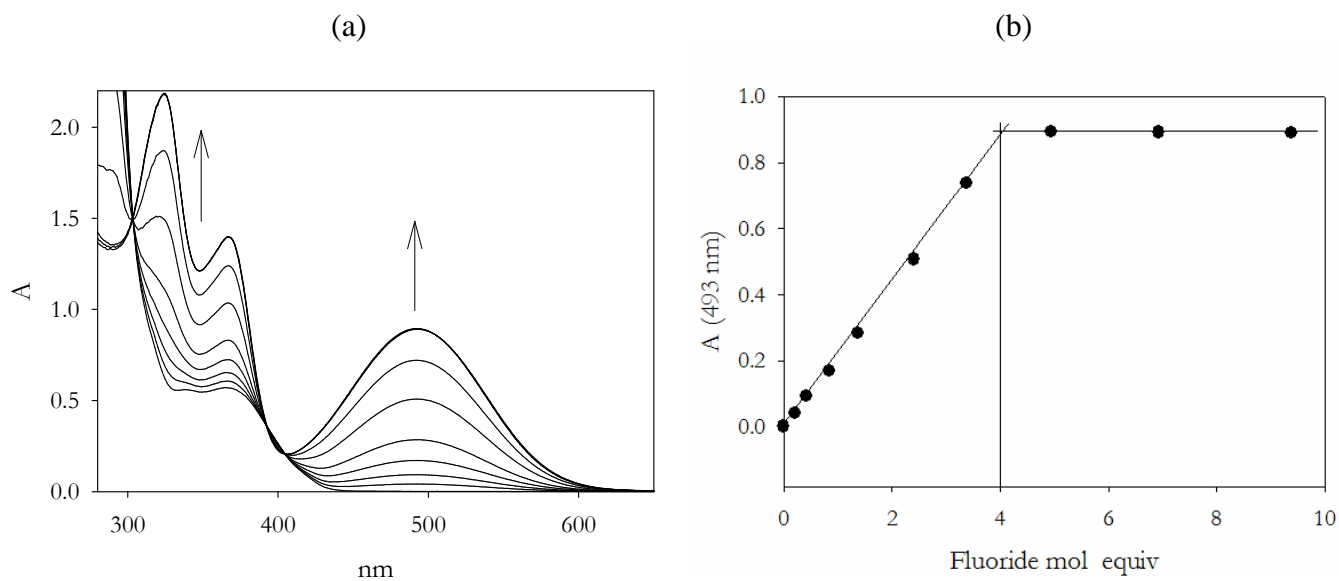


Figure S3: a) UV-Vis absorption changes of **2** (10.6×10^{-5} M) in DMSO upon addition of $[(\text{Bu})_4\text{N}]\text{F}$ at room temperature; b) plot of the absorbance at 493 nm vs. mol equiv of fluoride added. Lines show the equivalence reached at four equivalents.

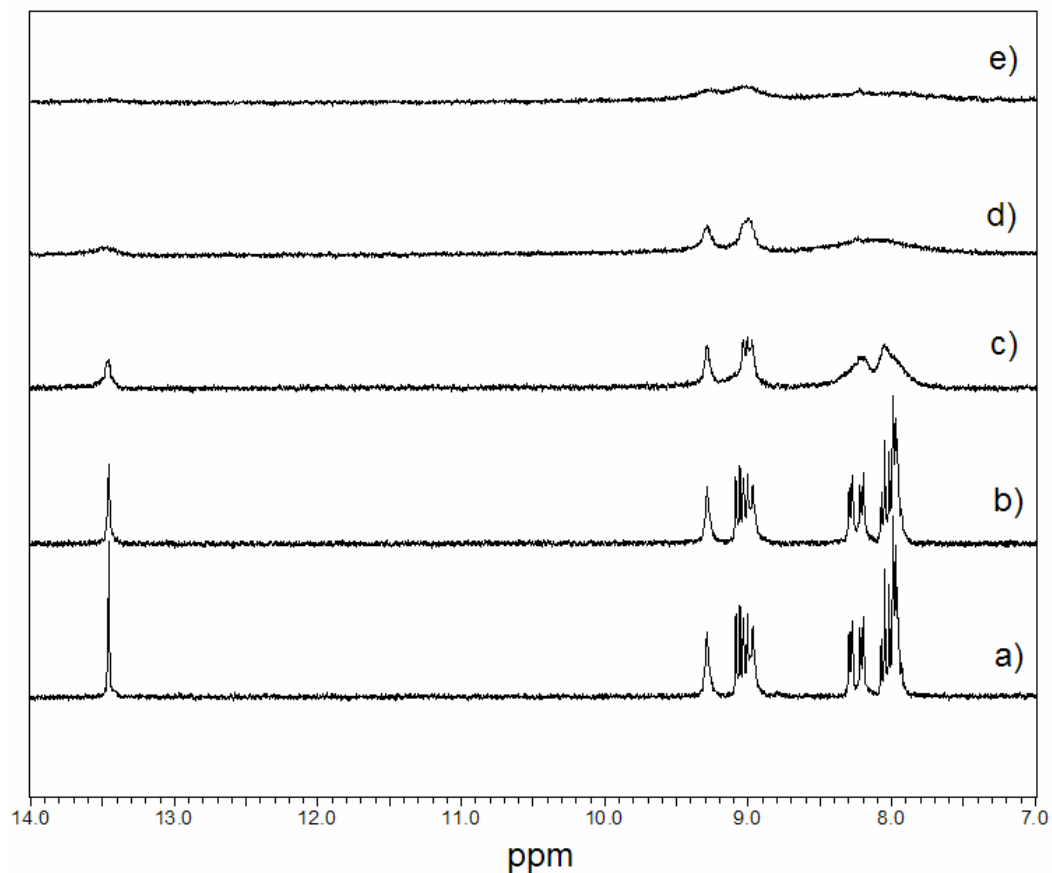


Figure S4: ^1H NMR (300 MHz) spectra of receptor **1** (5 mM) in $\text{DMSO-}d_6$ in the absence (a) and the presence of 0.2 (b), 0.4 (c), 0.6 (d) and 1.0 (e) equiv of $[(\text{Bu})_4\text{N}]\text{F}$ at room temperature (proton labeling shown in the Experimental section). Titration of **1** with F^- followed by ^1H -NMR showed the most progressive decrease of anthraquinone-NH signal at δ 13.45 ppm (compared to the signals of the side chain NH's) with no change of its chemical shift. Such changes are typical for deprotonation of NH group.^{S4} Additional changes in the spectra consist of broadening of signals due to multiple slow equilibria involved (NH \cdots F $^-$ interactions, resonance, possible Ar-CH \cdots F interactions).

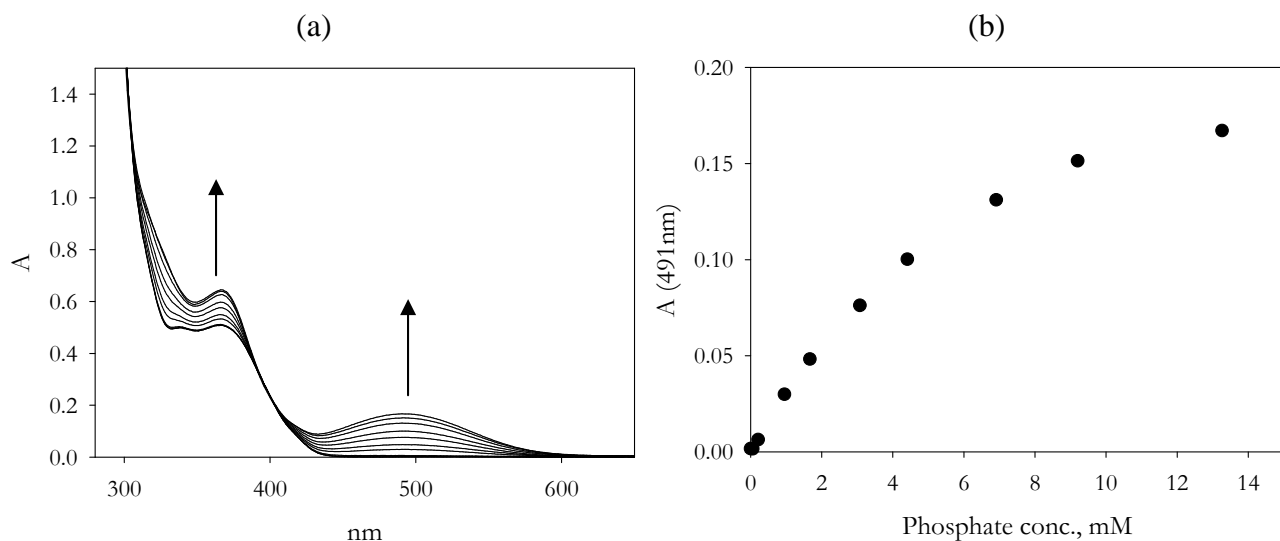


Figure S5: a) UV-Vis absorption changes of **2** (9.5×10^{-5} M) in DMSO upon addition of $[(\text{Bu})_4\text{N}]\text{H}_2\text{PO}_4$ at room temperature; b) plot of the absorbance at 491 nm vs. concentration of phosphate added.

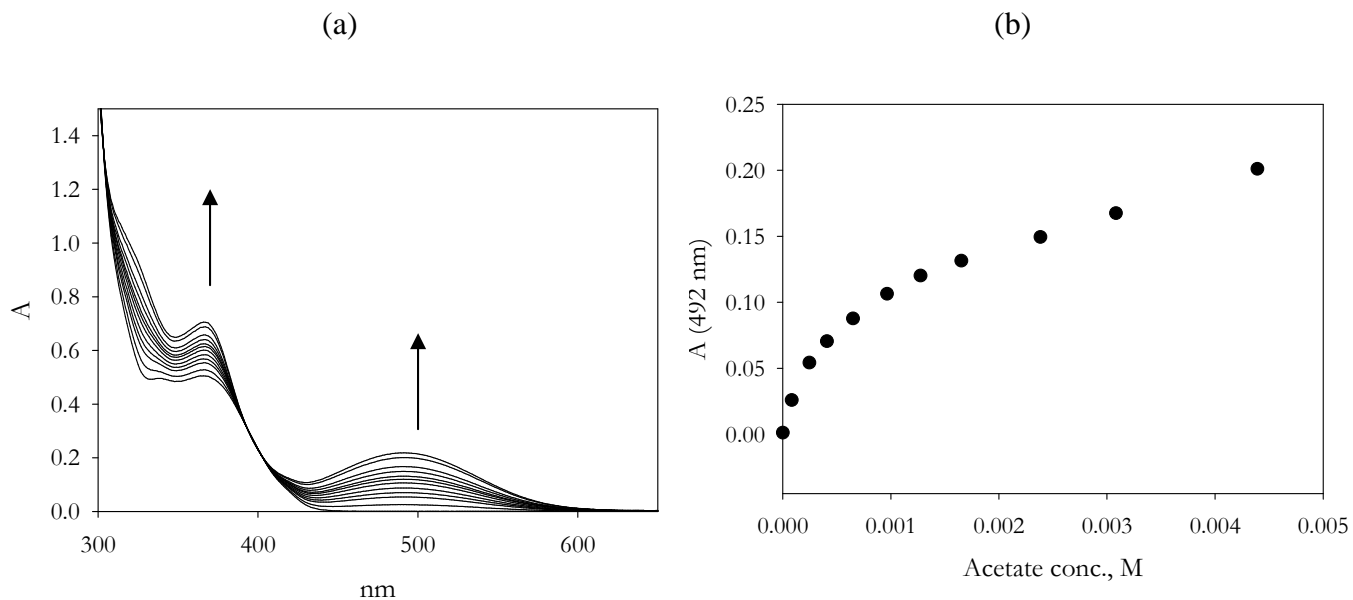
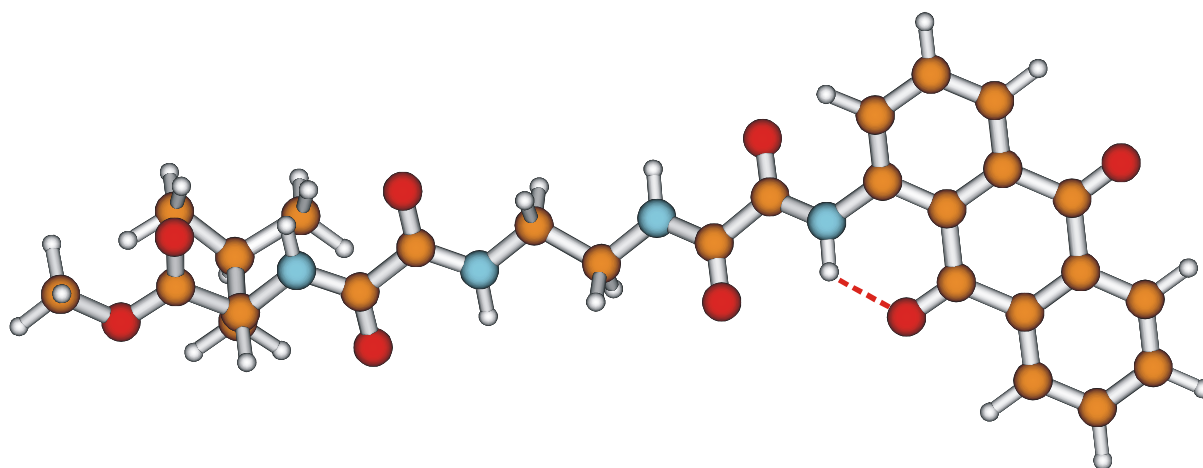
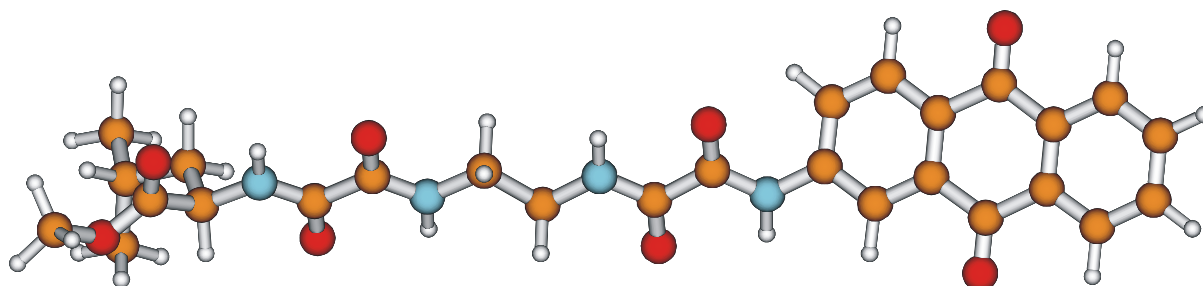


Figure S6: a) UV-Vis absorption changes of **2** (9.5×10^{-5} M) in DMSO upon addition of $[(\text{Bu})_4\text{N}]\text{CH}_3\text{COO}$ at room temperature; b) plot of the absorbance at 492 nm vs. concentration of acetate added.



1



2

Figure S7: Fully minimized structures of anthraquinone based oxalamide gelator **1** and its regioisomer **2** generated by systematic conformational search using SYBYL molecular modelling software of TRIPOS Inc.

Binding studies of the model compounds **3** and **4**

The families of spectra obtained upon addition of increasing amounts of fluoride, acetate and phosphate to a DMSO solution of **4** showed formation of a new band with a maximum around 480 nm. The experimental data at selected wavelengths can be easily fitted to a 1 : 1 binding isotherm to give a binding constants of $1.2 \times 10^5 \text{ M}^{-1}$ for fluoride, and 2.8×10^3 , and $5.3 \times 10^2 \text{ M}^{-1}$ for acetate and phosphate, respectively. Not surprisingly, fluoride is utterly the species with highest affinity, as also previously reported for similar kind of amidic receptors. Acetate and phosphate also bind to a lesser extent to **4**, in accordance with the observations for **2**. In contrast to **4**, compound **3** is not stable under the experimental conditions used and undergoes a side reaction to afford 1-aminoanthraquinone as showed by tlc and NMR comparison. The instability of **3** under the experimental conditions hampered any precise measurement. Anyway, we can estimate a binding constant in the order of 10^4 M^{-1} with fluoride (Fig. S11b, thick line) and at least two orders of magnitude lower for both acetate and phosphate anions.

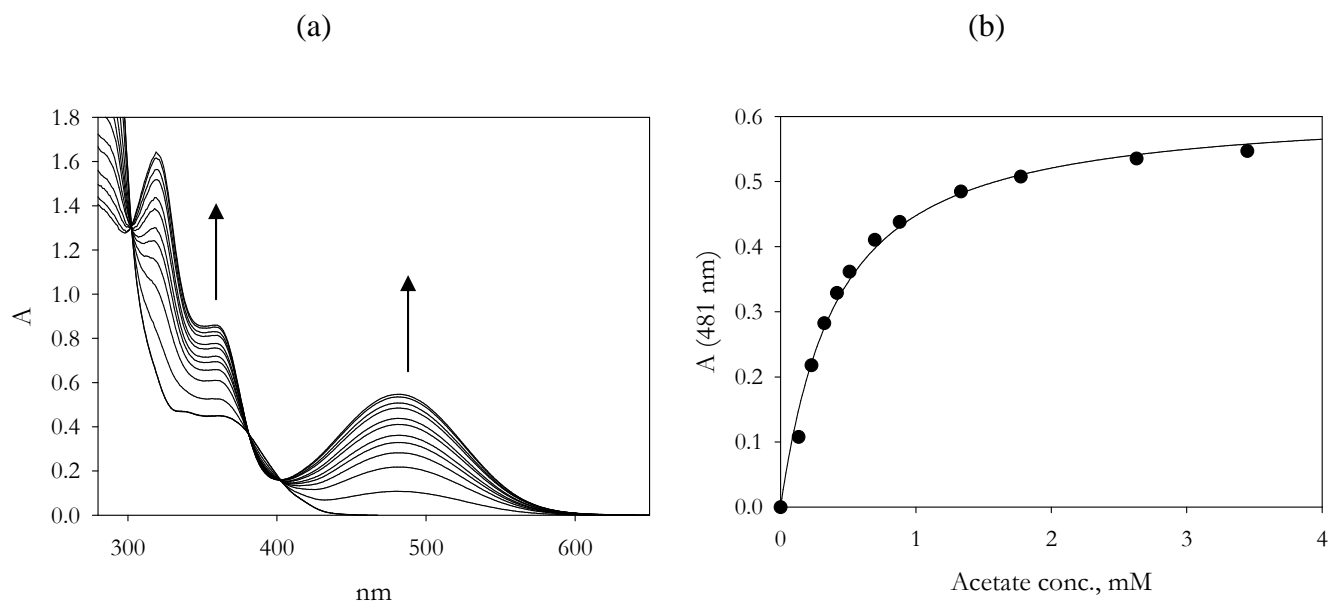


Figure S8: a) UV-Vis absorption changes of **4** (8.7×10^{-5} M) in DMSO upon addition of $[(\text{Bu})_4\text{N}]\text{CH}_3\text{COO}$ at room temperature; b) plot of the absorbance at 481 nm vs. concentration of acetate added.

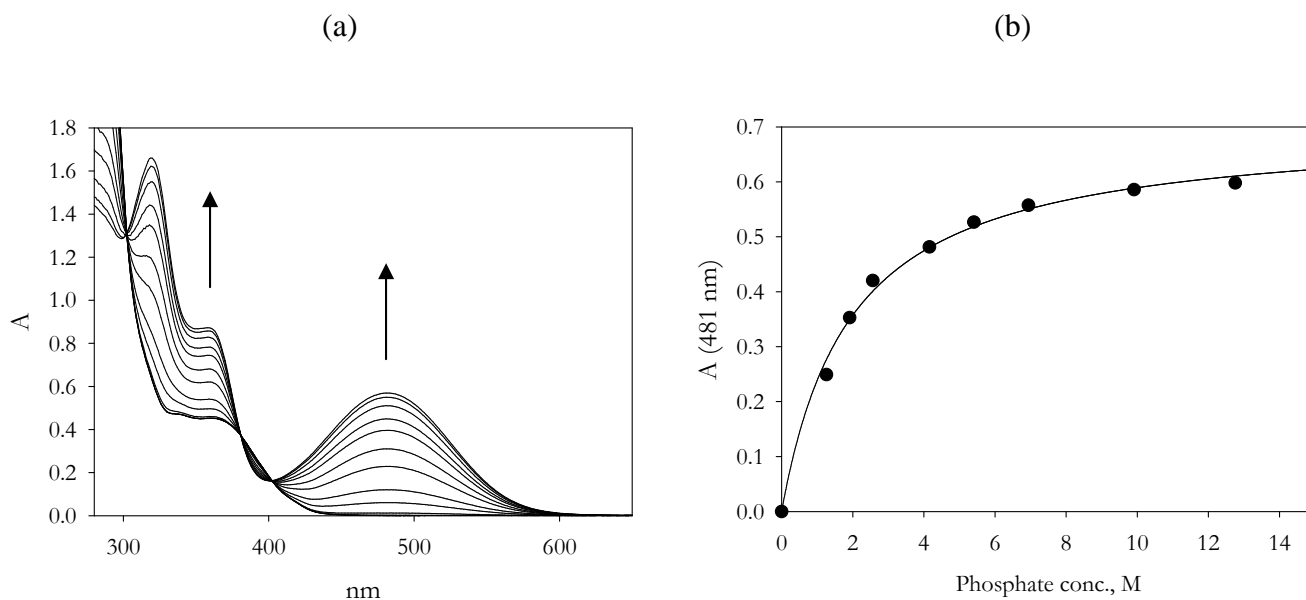


Figure S9: a) UV-Vis absorption changes of **4** (8.7×10^{-5} M) in DMSO upon addition of $[(\text{Bu})_4\text{N}]\text{H}_2\text{PO}_4$ at room temperature; b) plot of the absorbance at 481 nm vs. concentration of phosphate added.

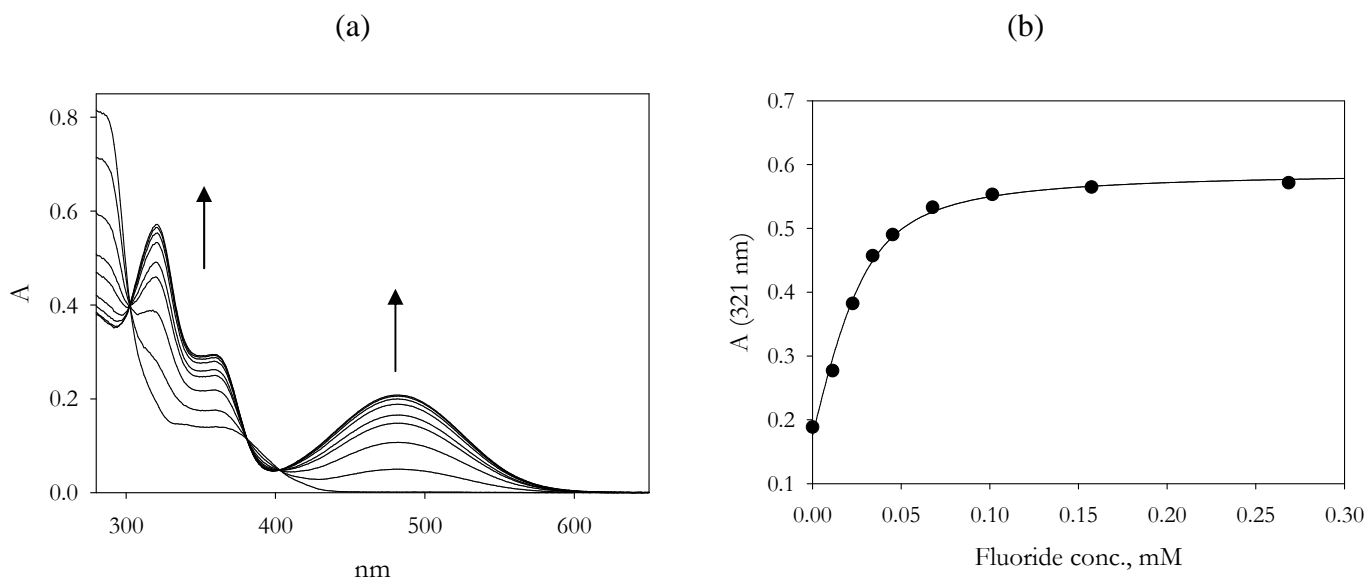


Figure S10: a) UV-Vis absorption changes of **4** (4.5×10^{-5} M) in DMSO upon addition of $[(\text{Bu})_4\text{N}]\text{F}$ at room temperature; b) plot of the absorbance at 321 nm vs. concentration of fluoride added.

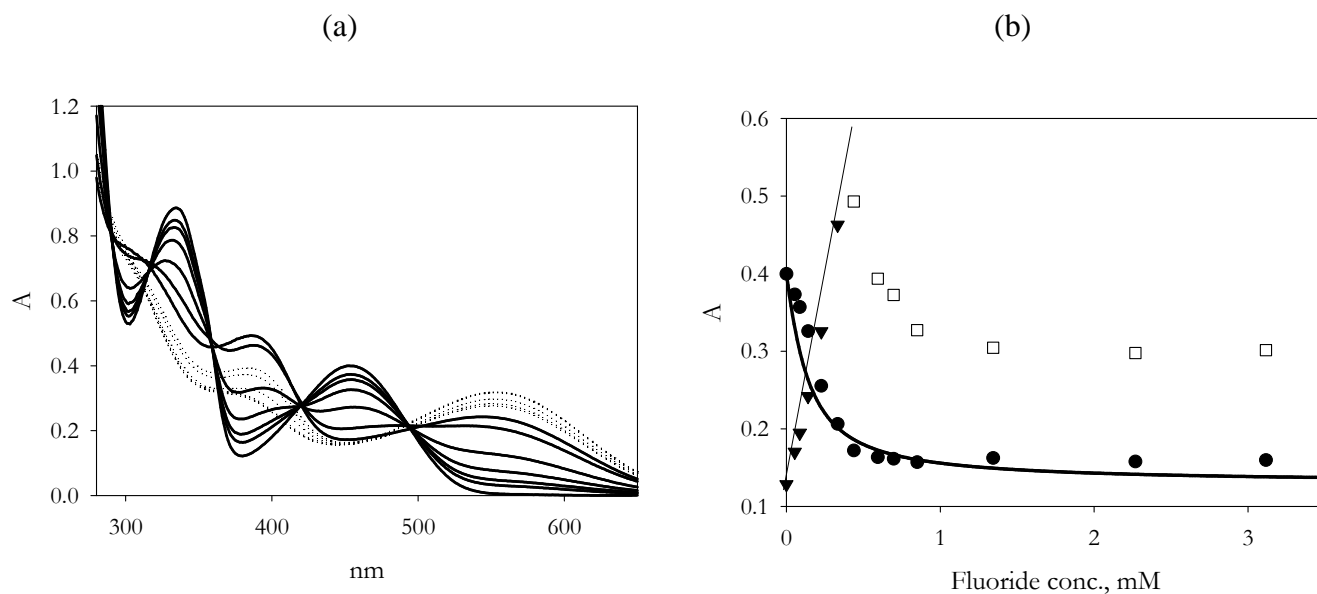


Figure S11: a) UV-Vis absorption changes of **3** (7.73×10^{-5} M) in DMSO upon addition of $[(\text{Bu})_4\text{N}]\text{F}$ at room temperature; b) plot of the absorbance vs. concentration of fluoride added (full triangle and open square: 385 nm; full circles: 335 nm; thick line: isothermal binding curve calculated for $K = 10^4 \text{ M}^{-1}$ and $\Delta\epsilon = 3440$).

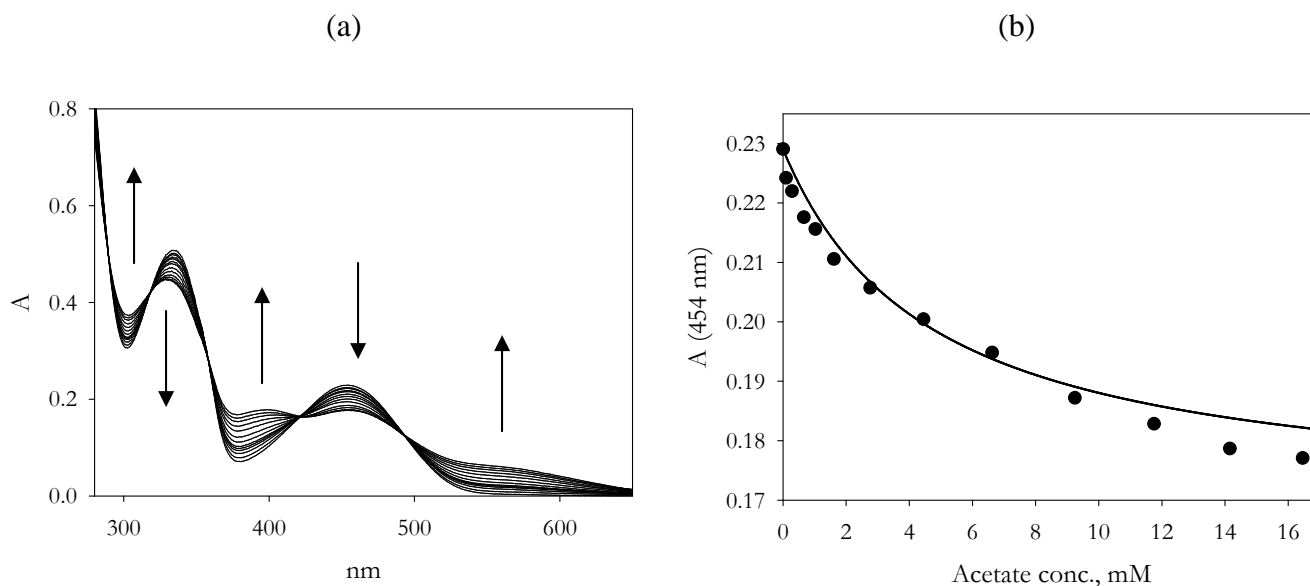


Figure S12: a) UV-Vis absorption changes of **3** (4.42×10^{-5} M) in DMSO upon addition of $[(\text{Bu})_4\text{N}]\text{CH}_3\text{COO}$ at room temperature; b) plot of the absorbance at 454 nm vs. concentration of acetate added (thick line: isothermal binding curve calculated for $K = 200 \text{ M}^{-1}$ and $\Delta\epsilon = 1450$).

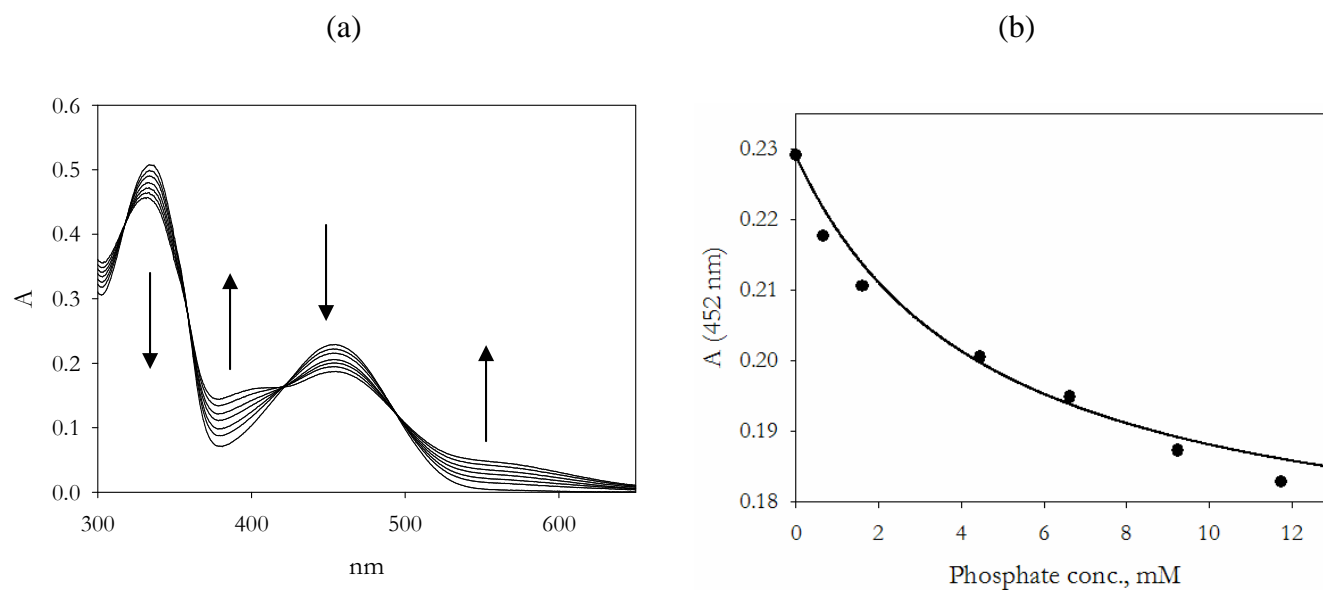


Figure S13: a) UV-Vis absorption changes of **3** (4.42×10^{-5} M) in DMSO upon addition of $[(\text{Bu})_4\text{N}]\text{H}_2\text{PO}_4$ at room temperature; b) plot of the absorbance at 452 nm vs. concentration of phosphate added (thick line: isothermal binding curve calculated for $K = 200 \text{ M}^{-1}$ and $\Delta\epsilon = 1400$).

Additional reference:

S1. I. Yavari, A. R. Alborzi, S. Dehghan and F. Nourmohammadian, *Phosphorus, Sulfur, and Silicon*, 2005, **180**, 625-631.

S2. P. A. Bezuglyi, L. M. Shtefan, N. S. Zhuravlev, Y. A. Golubenko, L. I. Filippova and S. M. Drogovoz, *Farm. Zh. (Kiev)*, 1985, **6**, 38-41, CAN 104:101953.

S3. C. M. Micklitsch, Q. Yu and J. P. Schneider, *Tetrahedron Lett.*, 2006, **47**, 6277-6280.

S4. Z. Lin, Y. Zhao, C. Duan, B. Zhang and Z. Bai, *Dalton Trans.*, 2006, 3678-3684.